

Weak antiferromagnetism of $J_{\text{eff}} = 1/2$ band in bilayer iridate $\text{Sr}_3\text{Ir}_2\text{O}_7$

S. Fujiyama,^{1,*} K. Ohashi,² H. Ohsumi,³ K. Sugimoto,⁴ T. Takayama,² T. Komesu,³ M. Takata,³ T. Arima,^{2,3} and H. Takagi^{5,1}

¹*RIKEN, Advanced Science Institute, Wako 351-0198, Japan*

²*Department of Advanced Materials, University of Tokyo, Kashiwa 277-8561, Japan*

³*RIKEN, SPring-8 Center, Sayo, Hyogo 679-5148, Japan*

⁴*JASRI, Sayo, Hyogo 679-5198, Japan*

⁵*Department of Physics, University of Tokyo, Hongo 113-0033, Japan*

(Dated: August 1, 2012)

The antiferromagnetic structure of $\text{Sr}_3\text{Ir}_2\text{O}_7$, the bilayer analogue of a spin-orbital Mott insulator Sr_2IrO_4 , was revealed by resonant magnetic x-ray diffraction. Contrasting intensities of the magnetic diffraction at the Ir L_{III} and L_{II} edges show a $J_{\text{eff}} = 1/2$ character of the magnetic moment as is argued in Sr_2IrO_4 . The magnitude of moment, however, was found to be smaller than that of Sr_2IrO_4 by a factor of 5-6, implying that $\text{Sr}_3\text{Ir}_2\text{O}_7$ is no longer a Mott insulator but a weak antiferromagnet. An evident change of the temperature dependence of the resistivity at T_N , from almost temperature-independent resistivity to insulating, strongly suggests that the emergent weak magnetism controls the charge gap. The magnetic structure was found to be an out-of-plane collinear antiferromagnetic ordering in contrast to the inplane canted antiferromagnetism in Sr_2IrO_4 , originating from the strong bilayer antiferromagnetic coupling.

Recently, novel interplay of spin-orbit coupling and electron correlations in heavy 5d transition metal oxides has been attracting considerable interest as a new paradigm of oxide physics. In Sr_2IrO_4 , a layered Ir^{4+} perovskite with five d -electrons in its t_{2g} orbitals, such interplay is particularly pronounced. Sr_2IrO_4 is an insulator with a charge gap of the order of $\lesssim 0.5$ eV and shows a canted antiferromagnetism below $T_N \sim 230$ K.¹⁻³ The insulating behavior even well above T_N and the presence of a large localized magnetic moment of $\sim 0.5\mu_B$, estimated from the large canted moment $0.075\mu_B/\text{Ir}$, indicate that Sr_2IrO_4 can be viewed as a Mott insulator. The Mottness of Sr_2IrO_4 is believed to be associated with a formation of a half-filled $J_{\text{eff}} = 1/2$ band, created by a very strong spin-orbit splitting as large as ~ 0.7 eV comparable to the width of the t_{2g} band ~ 1.5 eV. The polarization dependence of x-ray absorption spectra and the contrasting resonances at L_{II} and L_{III} edges in the magnetic x-ray diffraction firmly evidence $J_{\text{eff}} = 1/2$ character of the magnetic moment.³⁻⁵

The Mottness of Sr_2IrO_4 characterized by the charge gap as small as $\lesssim 0.5$ eV is marginal. Like some other tetravalent transition metal ions such as Ti^{4+} , Mn^{4+} and Ru^{4+} , Ir^{4+} forms a series of perovskite-based structures called Ruddlesden-Popper series, $\text{Sr}_{n+1}\text{Ir}_n\text{O}_{3n+1}$, with stacking of n - IrO_2 layers as structural units. Reflecting the marginal Mottness in Sr_2IrO_4 ($n = 1$), the system becomes more and more itinerant with increasing n . The three dimensional analogue of the series, SrIrO_3 ($n = \infty$) is known to show a metallic transport.⁶ Recent study revealed that the ground state of SrIrO_3 is a semimetal close to a band insulator,⁷ where the lifting of band degeneracy by spin-orbit coupling plays a key role in producing the incomplete charge gap.⁸ Very likely due to the presence of strong spin orbit coupling, the semimetal state is located almost right next to the Mott insulator. A question arises how the Mott insulator evolves into the

semimetal in $\text{Sr}_{n+1}\text{Ir}_n\text{O}_{3n+1}$.

$\text{Sr}_3\text{Ir}_2\text{O}_7$, the $n = 2$ member of $\text{Sr}_{n+1}\text{Ir}_n\text{O}_{3n+1}$, could be a key compound to pursue the electronic evolution from the spin-orbital Mott insulator to the semimetal. As shown in Fig. 1 (a), the crystal structure consists of stacking of bilayers of corner-shared IrO_6 octahedra along the c -axis. The octahedra are rotated around the c -axis and the inplane Ir-O-Ir bonds are hence bent. The directions of the rotations are opposite for the neighboring IrO_6 octahedra not only within each layer but also between the two layers. $\text{Sr}_3\text{Ir}_2\text{O}_7$ is reported to show a semiconducting temperature dependence of the resistivity but much more conducting than Sr_2IrO_4 , implying close proximity to the critical border to the semimetal.⁹⁻¹¹ A very weak ferromagnetic moment was observed in the temperature dependent magnetization below 280 K, suggesting the presence of magnetic ordering, but the magnetic structure has not been fully explored yet. By determining the magnetic structure of $\text{Sr}_3\text{Ir}_2\text{O}_7$, we should be able to address the following issues closely linked to the evolution of the electronic state from the Mott insulator to the semimetal.

Is the $J_{\text{eff}} = 1/2$ state robust against the change of the crystal structure and the itinerancy of the electrons? The ratios of the inplane and out-of-plane Ir-O bond lengths are 1.04 for Sr_2IrO_4 and 1.02 for $\text{Sr}_3\text{Ir}_2\text{O}_7$, implying less distorted IrO_6 octahedra.⁹ Assuming a comparable spin-orbit coupling to Sr_2IrO_4 , we may anticipate a formation of almost ideal $J_{\text{eff}} = 1/2$ state. However, it is highly nontrivial whether the increased itinerancy could destabilize the $J_{\text{eff}} = 1/2$ state, which should be examined experimentally. Even if the $J_{\text{eff}} = 1/2$ character holds for $\text{Sr}_3\text{Ir}_2\text{O}_7$, the estimate of the magnitude of the ordered moment will provide a key to examine the Mottness of this material.

The magnetic structure of this material should be pinned down. The rotational distortion of the IrO_6 oc-

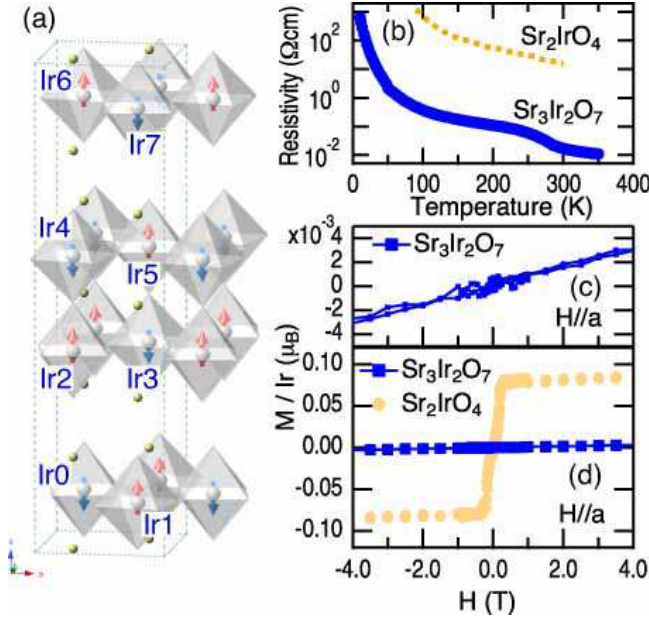


FIG. 1. (a) The crystal and magnetic structures of $\text{Sr}_3\text{Ir}_2\text{O}_7$. The dashed line denotes the unit cell. Note that the volume of the magnetic unit cell agrees to that of the lattice. We label eight iridium sites (grey circles, Ir_j , $j = 0 \dots 7$) for the following analysis of the magnetic structure. (b) Inplane resistivities of $\text{Sr}_3\text{Ir}_2\text{O}_7$ and Sr_2IrO_4 . (c) and (d) Magnetizations of $\text{Sr}_3\text{Ir}_2\text{O}_7$ at 260 K and Sr_2IrO_4 at 5 K¹⁵.

tahedra, alternating in each plane and opposite between the upper and the lower layers, could give rise to a net ferromagnetic canting moment when antiferromagnetically coupled moments are lying in the plane through Dzyaloshinskii-Moriya (DM) interaction as is argued in Sr_2IrO_4 . On the other hand, the intrabilayer coupling, J_\perp , that is absent in Sr_2IrO_4 and perhaps antiferromagnetic that is comparable or even larger than that within the plane could conflict with the inplane canted moments. The reported weak ferromagnetic moment of $\text{Sr}_3\text{Ir}_2\text{O}_7$ was in fact only 1% of that of Sr_2IrO_4 ($< 10^{-3}\mu_B/\text{Ir}$) and showed very peculiar temperature dependence.⁹ We suspect that this could be originating from an extrinsic moment produced by defects.

In this communication, we report the magnetic structure of the bilayer perovskite, $\text{Sr}_3\text{Ir}_2\text{O}_7$, determined by resonant magnetic x-ray diffraction. The magnetic structure was found to be collinear along the c -axis with antiferromagnetic intrabilayer coupling, in marked contrast to the inplane canted antiferromagnetism in Sr_2IrO_4 . We found that the ordered moment below $T_N = 280$ K has a $J_{\text{eff}} = 1/2$ character but that the magnitude is substantially reduced to 1/5-1/6 of that of Sr_2IrO_4 , which points out that $\text{Sr}_3\text{Ir}_2\text{O}_7$ is a $J_{\text{eff}} = 1/2$ band magnetic semiconductor rather than a $J_{\text{eff}} = 1/2$ Mott insulator.

A single crystal of $\text{Sr}_3\text{Ir}_2\text{O}_7$ with a dimension of $2\text{ mm} \times 2\text{ mm} \times 0.5\text{ mm}$ was synthesized by a flux method. The resistivity measurement was conducted by a conventional four probe technique. The magnetization measure-

TABLE I. Atomic positions of $\text{Sr}_3\text{Ir}_2\text{O}_7$ determined by synchrotron radiation x-ray diffraction at 295 K.

| atom | x | y | z |
|------|--------|--------|--------|
| Ir | 0.2500 | 0.7500 | 0.0974 |
| Sr1 | 0.2500 | 0.2500 | 0.0000 |
| Sr2 | 0.2500 | 0.2500 | 0.2500 |
| O1 | 0.2500 | 0.7500 | 0.0000 |
| O2 | 0.2500 | 0.7500 | 0.1943 |
| O3 | 0.5487 | 0.5485 | 0.0962 |

ment was performed using a commercial SQUID magnetometer. A single crystal x-ray diffraction measurement for the determination of the lattice structure was performed using a cylindrical IP (imaging plate) on BL02B1 at SPring-8.¹² The wavelength of the incident x-ray was set to 0.354 \AA . Resonant magnetic diffraction measurement using a multi-circle diffractometer was performed on BL19LXU of SPring-8.¹³ The wavelength was set to 1.106 \AA corresponding to the L_{III} edge ($2p_{3/2} \rightarrow 5d$) of iridium for the magnetic structure analysis. The b -axis of the crystal was nearly kept parallel to the scattering plane.

The analysis of the crystal structure indicates an orthorhombic structure with the space group $Bbeb$ and the lattice constants of 5.5108 , 5.512 , 20.8832 \AA , that has lower symmetry than $I\bar{4}/mmm$ that is reported at very early stage,¹⁰ but agrees to more recent analysis.⁹ The result of structural refinement is shown in Table I. We found that the presence of the two domains associated with orthorhombic distortion and that the ratio of the volumes of the two domains was roughly $0.7:0.3$. In the magnetization of the crystal measured, a very weak ferromagnetism was observed below 280 K only when the inplane magnetic field was applied. The magnitude of moment, however, is almost 1% of that of Sr_2IrO_4 as shown in Fig. 1(c) and (d), in agreement with the previous report. On the other hand, the reported peculiar reduction of the susceptibility below 50 K was not reproduced.⁹ Additional weak ferromagnetic signal was observed below 230 K , which we attribute to the intergrowth of Sr_2IrO_4 layer.¹⁴ From the magnetization measurement, we estimate that the intergrowth is 1 % of the total volume. The resistivity of the crystal in Fig. 1(b) showed a semiconducting temperature dependence. An evident anomaly at the magnetic transition temperature is observed suggestive of a close interrelation between the magnetism and the motion of electrons. Above the magnetic transition temperature, $T_N \sim 280\text{ K}$, the magnitude of the resistivity is as low as $\rho \sim 10\text{ m}\Omega\text{cm}$ and weakly temperature dependent. This suggests that the system is a poor metal or a very narrow gap semiconductor at high temperatures.

How about magnetism? We found the $(0\ 1\ 13)$ reflection in the IP at 30 K when the incident wavelength of x-ray was tuned at the L_{III} edge of iridium, that is prohibited in a B -base centered lattice and apparently shows an

inplane antiferromagnetism. To elucidate the magnetic correlation along the c -axis, particularly the unknown intralayer coupling, we performed a resonant magnetic x-ray diffraction experiment by a four-circle diffractometer for $(0\ 1\ l)$ reflections. The magnetic diffraction evolves below 280 K as shown in Fig. 2 (b), which evidences that the anomaly in the magnetization originates from the antiferromagnetic long range ordering. Upon cooling, the magnetic diffraction evolves monotonously, excluding a possibility of the second magnetic transition at ~ 230 K. The magnetic diffraction that is normalized by the intensity of the charge diffraction ($I_m(0\ 1\ 13)/I_c(0\ 0\ 20)$) is reduced to nearly 1/150 to that of a spin-orbital Mott insulator Sr_2IrO_4 ($I_m(1\ 0\ 22)/I_c(0\ 0\ 24)$) as shown in Fig. 2 (a) plausibly originating from the itinerant character of electrons. It is to be noted that the structure factors of the charge diffractions, F_{0020} of $\text{Sr}_3\text{Ir}_2\text{O}_7$ and F_{0024} of Sr_2IrO_4 , have nearly the same magnitudes. Despite the contrasting difference in the diffraction intensities, the ordered moment keeps a $J_{\text{eff}} = 1/2$ character like Sr_2IrO_4 evidenced by the strong enhancement at the L_{III} edge as shown in Fig. 2 (c).

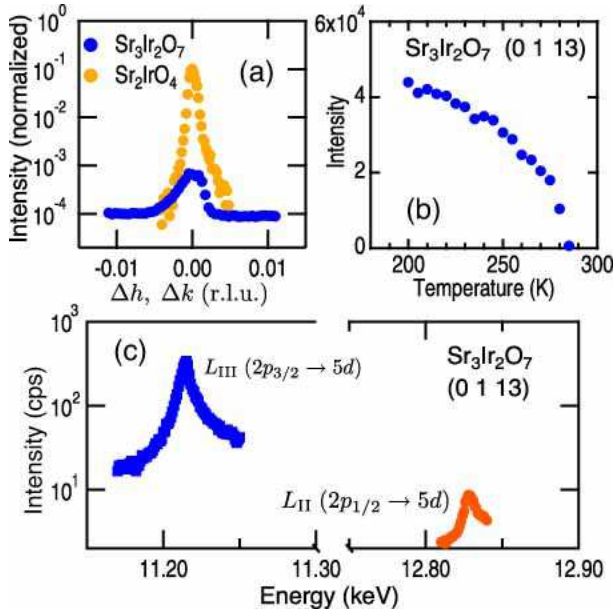


FIG. 2. (a) The resonant magnetic diffraction normalized by the charge scattering of Sr_2IrO_4 ($I_m(1\ 0\ 22)/I_c(0\ 0\ 24)$) and $\text{Sr}_3\text{Ir}_2\text{O}_7$ ($I_m(0\ 1\ 13)/I_c(0\ 0\ 20)$). (b) Temperature evolution of the magnetic diffraction $(0\ 1\ 13)$. (c) Strong enhancement of the diffraction at the L_{III} edge ($c\hbar/\lambda = 11.2$ keV) is observed while only small diffraction is observed at the L_{II} edge ($c\hbar/\lambda = 12.8$ keV).

We show in Fig. 3 (a) the l dependence of the magnetic diffraction. Under the resonance condition at the L edge, the diffraction intensity is described as,

$$I(hkl) \propto |(\epsilon' \times \epsilon) \cdot \mathbf{m}|^2 |F_{hkl}|^2 = |(\epsilon_{\pi'} \times \epsilon_{\sigma}) \cdot \mathbf{m}|^2 |F_{hkl}|^2,$$

where $\epsilon(\epsilon')$ is the polarization vector of the incident

(scattered) x-ray, $\mathbf{m} = m_a \hat{e}_a + m_b \hat{e}_b + m_c \hat{e}_c$ is the ordered moment and F_{hkl} denotes the structure factor.

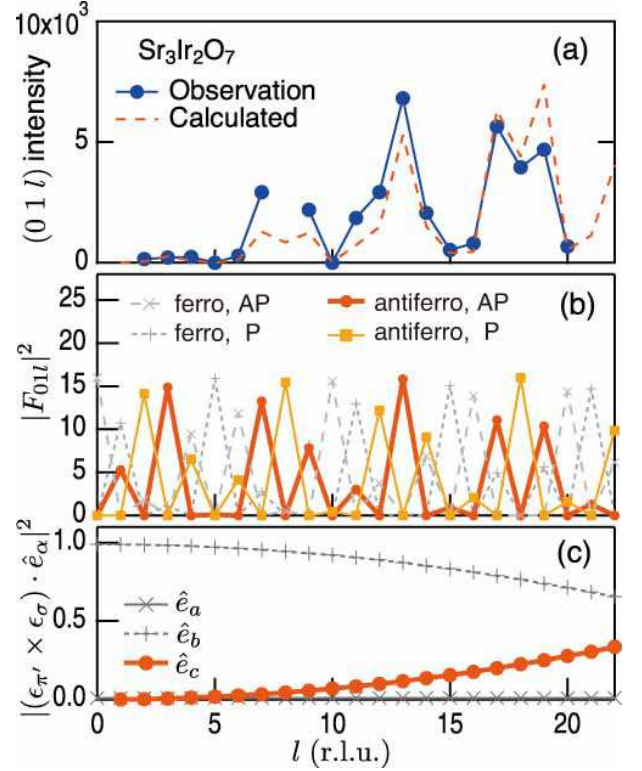


FIG. 3. (a) Intensities of the resonant magnetic x-ray diffraction at $(0\ 1\ l)$ (blue circle). We encountered a technical difficulty in measuring $(0\ 1\ 8)$ reflection by the geometry of the diffractometer, and this is missing. Orange dashed line is the calculated intensity for the antiferromagnetic intralayer coupling with moment parallel to the c -axis assuming a mixture of 90° rotated domains by a factor of 0.7 to 0.3. See the detail in the text. (b) Calculated $|F_{01l}|^2$ of four possible magnetic structures with intralayer magnetic couplings ($f_4 = \pm f_2$) and interbilayer antiparallel (AP) and parallel (P) relations ($f_0 = \mp f_2$). (c) The $|(\epsilon_{\pi'} \times \epsilon_{\sigma}) \cdot \hat{e}_\alpha|^2$ for $\hat{e}_\alpha \parallel a, b$ and c .

A continuous l scan along $(0\ 1\ l)$ detects no magnetic superspot, which shows that the magnetic periodicity along the c -direction agrees to the c of the unit cell containing four IrO_6 layers. When we denote the direction (sign) of the moment at $\text{Ir}j$ site as $f_j (j = 0 \dots 7)$ (Fig. 1 (a)) under a condition of inplane antiferromagnetism for each IrO_2 plane evidenced by the IP measurement as, $f_{1(3,5,7)} = -f_{0(2,4,6)}$, the squared structure factor at $(0\ 1\ l)$ is calculated as,

$$|F_{01l}|^2 = 4[\sin^2 \theta (f_0 - f_6 + (-1)^l f_2 - (-1)^l f_4)^2 + \cos^2 \theta (-f_0 - f_6 + (-1)^l f_2 + (-1)^l f_4)^2],$$

using $\theta = 2\pi \cdot 0.0974 \cdot l$.

The possible magnetic structures are limited to 4 cases depending on the intralayer magnetic couplings (J_\perp , $f_4 = \pm f_2$ for ferromagnetic (antiferromagnetic)) and the

interbilayer relations ($f_0 = \mp f_2$ for antiparallel (parallel)), of which $|F_{01l}|^2$ are plotted in Fig. 3 (b). The sign of J_\perp determines the phase of the overall l dependence with a periodicity of $1/(2 \cdot 0.0974) = 5.13$, and the plot in Fig. 3 (b) apparently shows an antiferromagnetic intrabilayer coupling.

The smearing-out of the even-odd alternating l -dependence of the observed diffraction is originating from the presence of two structural domains in the crystal. Using the ratio of the domains of 0.7 to 0.3 deduced by the crystal structure analysis, the observed intensity is expected as $I(01l) \propto 0.7|(\epsilon_{\pi'} \times \epsilon_{\sigma'}) \cdot \hat{e}_\alpha|^2 |F_{01l}|^2 + 0.3|(\epsilon_{\pi'} \times \epsilon_{\sigma'}) \cdot \hat{e}_\beta|^2 |F_{10l}|^2$, where \hat{e}_β should be 90° rotated to \hat{e}_α around the c -axis.¹⁶ The calculated $|(\epsilon_{\pi'} \times \epsilon_{\sigma'}) \cdot \hat{e}_\alpha|^2$ for $\alpha = a, b$ and c show contrasting l dependences as well as the magnitudes as shown in Fig. 3 (c). Under the condition of the sample orientation with b -axis parallel to the scattering plane, the $m_a \hat{e}_a$ gives negligible contribution to the diffraction because of $\epsilon_{\sigma'} \parallel \hat{e}_a$. The only choice of the unit vectors to smear out the even-odd alternation is $\hat{e}_\alpha = \hat{e}_\beta = \hat{e}_c$, therefore, we conclude that the ordered moments are directed along the c -axis.¹⁷ We plot in Fig. 3 (a) the calculated l dependence of the diffraction considering the structural domains and c -directed moments with antiferromagnetic J_\perp , which shows a good agreement with the observed magnetic diffraction. The determined magnetic structure as shown in Fig. 1 (a) well resolves the absence of weak ferromagnetic moment and the negligible magnetization below T_N ($< 0.001 \mu_B$ at 260 K), because the moments lie parallel to the DM vectors.

The most plausible source to realize the collinear magnetic structure along the c -axis is the antiferromagnetic J_\perp . In contrast to the inplane Ir-O-Ir bond that is bent with 11° , the straight bond along the out-of-plane direction connecting two layers with nearly the same distance expects a considerable J_\perp with nearly the same or even larger than the inplane antiferromagnetic exchange. We consider that this large J_\perp can conflict with the DM interaction favoring inplane canting of the moments, and as a consequence to avoid the competition, the moments are directed parallel to the DM vectors.

The observed magnetic diffraction normalized by the charge diffraction is nearly 150 times smaller than that of Sr_2IrO_4 . Even considering the reduction of the diffraction intensity originating from the difference of the directions of the moments by a factor of $[|(\epsilon_{\pi'} \times \epsilon_{\sigma'}) \cdot \hat{e}_a|^2 \text{ at } (1\ 0\ 22)]/[|(\epsilon_{\pi'} \times \epsilon_{\sigma'}) \cdot \hat{e}_c|^2 \text{ at } (0\ 1\ 13)] \sim 5$, a strong reduction of the squared moment $|m_c(\text{Sr}_3\text{Ir}_2\text{O}_7)|/m_a(\text{Sr}_2\text{IrO}_4)|^2 \sim 1/30$ is suggested. While the magnitudes of the ordered moments of different samples cannot precisely be determined solely by resonant x-ray diffraction, the moment of $\text{Sr}_3\text{Ir}_2\text{O}_7$ is considerably reduced to $1/5$

- $1/6$ of that of Sr_2IrO_4 , i.e. $\sim 0.1 \mu_B/\text{Ir}$. The reduced magnetic moment clearly shows that the magnetism of $\text{Sr}_3\text{Ir}_2\text{O}_7$ should be better described by a band magnetism of $J_{\text{eff}} = 1/2$ electrons rather than a Mott insulator. The anomaly in the resistivity is very clearly observed at T_N , implying the band magnetism is controlling the poor-metal insulator transition. One may argue the possibility of the formation of a Slater insulator or an SDW state below T_N .¹⁸ We, however, note that the magnetic structure revealed has the same unit cell as the unit cell of the lattice and a band folding associated with the antiferromagnetic ordering would not be anticipated. In this respect, neither Slater nor SDW scenario in their most naive form can be applied here and much more elaborated picture should be invoked. It is interesting to note here again the contrast between Sr_2IrO_4 and $\text{Sr}_3\text{Ir}_2\text{O}_7$. Only a minute change in the crystal structure alters the system from a strongly localized magnet to a weakly localized band magnet, which we believe represents a extremely delicate interplay of Coulomb U , kinetic energy t , spin-orbit coupling and lattice.

In conclusion, we disclosed the antiferromagnetic structure of the bilayer perovskite iridium oxide, $\text{Sr}_3\text{Ir}_2\text{O}_7$, by resonant magnetic x-ray diffraction. Despite much more itinerant character of electrons than the spin-orbital Mott insulator, Sr_2IrO_4 , $J_{\text{eff}} = 1/2$ electronic state holds for this material. The ordered magnetic moment is directed along the c -axis, which explains the absence of the remnant ferromagnetic moment, plausibly originating from the competition of the intrabilayer antiferromagnetic exchange and the Dzyaloshinskii-Moriya interaction. Apart from the resemblance of the antiferromagnetism and T_N to Sr_2IrO_4 , the ordered moment is strongly reduced down to nearly $1/5$ to that of Sr_2IrO_4 , showing that the electronic state is no longer a Mott insulator but a band magnet. A considerable interplay between the magnetism and the transport is demonstrated, where the emergent moment appears to control the transition from a poor metal (narrow gap semiconductor) to an insulator. In the course of this study, we noticed a result of magnetic x-ray diffraction of this sample.¹⁹ The magnetic structure proposed is consistent with the current study.

ACKNOWLEDGMENTS

We are grateful to W. Koshibae, D. Hashizume, H.Y. Kee, G. Khaliullin, and G. Jackeli for fruitful discussions. The synchrotron radiation experiments were performed at BL19LXU in SPring-8 with the approval of RIKEN (20080047). This work was supported by Grant-in-Aid for Scientific Research on Priority Areas (19052007, 17071001) from MEXT.

* fujiyama@riken.jp

¹ M.K. Crawford, M.A. Subramanian, R.L. Harlow, J.A.

- Fernandez-Baca, Z.R. Wang, and D.C. Johnston, Phys. Rev. B **49**, 9198 (1994).
- ² G. Cao, J. Bolivar, S. McCall, and J.E. Crow, and R. P. Guertin, Phys. Rev. B **57**, R11039 (1998).
 - ³ B.J. Kim, Hosub Jin, S.J. Moon, J.-Y. Kim, B.-G. Park, C.S. Leem, Jaejun Yu, T.W. Noh, C. Kim, S.-J. Oh, J.-H. Park, V. Durairaj, G. Cao, and E. Rotenberg, Phys. Rev. Lett. **101**, 076402 (2008).
 - ⁴ B.J. Kim, H. Ohsumi, T. Komesu, S. Sakai, T. Morita, H. Takagi, and T. Arima, Science **323** 1329 (2009).
 - ⁵ S. Fujiyama, H. Ohsumi, T. Komesu, J. Matsuno, B.J. Kim, M. Takata, T. Arima, and H. Takagi, Phys. Rev. Lett. **108**, 247212 (2012).
 - ⁶ G. Cao, V. Durairaj, S. Chikara, L.E. DeLong, S. Parkin, and P. Scholttmann, Phys. Rev. B, **76**, 100402 (2007).
 - ⁷ T. Takayama *et al.* in preparation.
 - ⁸ Jean-Michel Carter, V. Vijay Shankar, M. Ahsan Zeb, and Hae-Young Kee, Phys. Rev. B, **85**, 115105 (2012).
 - ⁹ G. Cao, Y. Xin, C.S. Alexander, J.E. Crow, P. Schlottmann, M.K. Crawford, R.L. Harlow, and W. Marshall, Phys. Rev. B **66**, 214412 (2002).
 - ¹⁰ M.A. Subramanian, M.K. Crawford, and R.L. Harlow, Mater. Res. Bull. **29**, 645 (1994).
 - ¹¹ I. Nagai, Y. Yoshida, S.I. Ikeda, H. Matsuhata, H. Kito, and M. Kosaka, J. Phys: Cond. Mat. **19**, 136214 (2007).
 - ¹² K. Sugimoto, H. Ohsumi, S. Aoyagi, E. Nishibori, C. Moriyoshi, Y. Kuroiwa, H.i Sawa, and M. Takata, AIP Conf. Proc. **1234**, 887 (2010).
 - ¹³ M. Yabashi *et al.* Nuc. Inst. Meth. Phys. Res. A **467-468**, 678 (2001).
 - ¹⁴ The following paper reports an antiferromagnetic structure of $\text{Sr}_3\text{Ir}_2\text{O}_7$, but the magnetic diffraction appears below 230 K, showing a contradiction to our results. S. Boseggia, R. Springell, H.C. Walker, A.T. Boothroyd, D. Prabhakaran, D. Wermeille, L. Bouchenoire, S.P. Collins, and D.F. McMorrow, Phys. Rev. B **85**, 184432 (2012).
 - ¹⁵ Since our single crystal of $\text{Sr}_3\text{Ir}_2\text{O}_7$ contains the intergrowth of Sr_2IrO_4 , we show the magnetization data at 260 K, 20 K below T_N . We consider nearly half of the saturated magnetization develops at 260 K.
 - ¹⁶ The $|F_{01l}|^2$ for $f_0 = -f_2$ agrees to $|F_{10l}|^2$ for $f_0 = f_2$.
 - ¹⁷ Mathematically, there remains a possibility of $m_a = m_b$ corresponding to the direction of moments to $\hat{e}_a + \hat{e}_b$, however, this magnetic structure could not be realized in an orthorhombic lattice. In addition, inplane moments meet a significant conflict to the magnetization as discussed below.
 - ¹⁸ R. Arita, J. Kunes, A.V. Kozhevnikov, A.G. Eguiluz, and M. Imada, Phys. Rev. Lett. **108**, 086403 (2012).
 - ¹⁹ J.W. Kim, Y. Choi, Jungho Kim, J.F. Mitchell, G. Jackeli, M. Daghofer, J. van den Brink, G. Khaliullin, and B.J. Kim, Phys. Rev. Lett. **109**, 037204 (2012).